INTERACTIVE CONTROL ENGINEERING
Principles and Applications

Volume 17 Control of Energy Conversion and Storage

CHAPTER 5

Energy-Maximizing Control of a Heaving Buoy on a Fading Wave Forecast

Pages 111–133

Edited by John D. Hedengren

How to cite this chapter. "Energy-Maximizing Control of a Heaving Buoy on a Fading Wave Forecast," in *Control of Energy Conversion and Storage*, John D. Hedengren, Ed., vol. 17 of *Interactive Control Engineering: Principles and Applications*. Advanced Process Solutions, LLC, 2026, ch. 5, pp. 111–133.

The page numbers in this file are those of the printed volume.

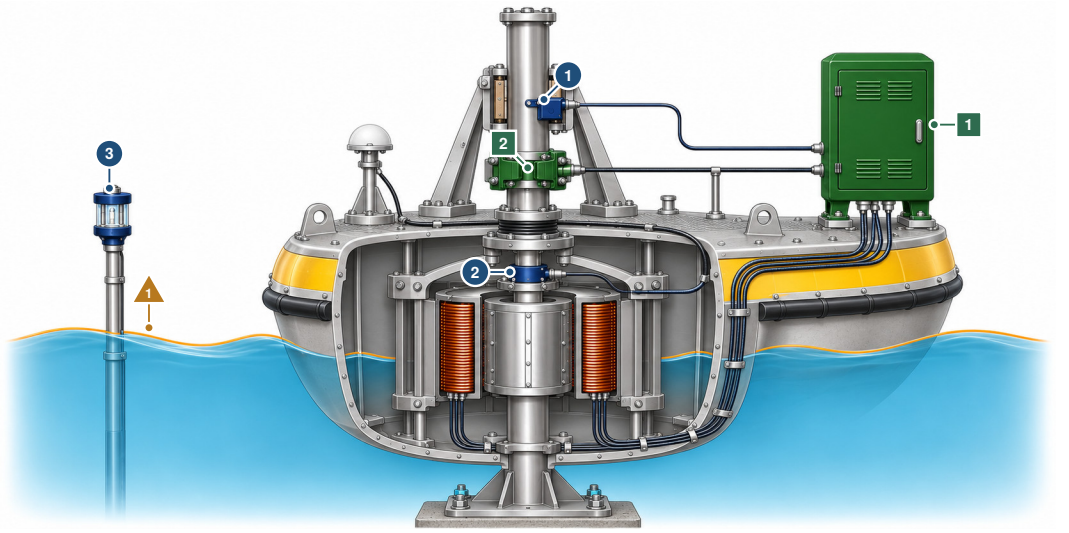
The app for this chapter
https://apmonitor.com/apps/wave-energy/

The volume online: contents, other chapters and citation records
https://apmonitor.com/apps/books/v17-energy/#wave-energy

Copyright © 2026 Advanced Process Solutions, LLC. All rights reserved. Produced by Advanced Process Solutions, LLC.

CHAPTER 5

Energy-Maximizing Control of a Heaving Buoy on a Fading Wave Forecast



The controller moves 1 drive that sets the generator's force 2 brake that holds the buoy still

The controller reads 1 position and speed of the buoy on the spar 2 force between buoy and generator 3 wave probe upstream of the buoy

What disturbs it 1 the waves and the force they exert

Notice that the controller reads the buoy's motion, the force on its generator and the sea at a probe upstream, but never the wave force on the buoy itself, which it must estimate and forecast. Illustration, not to scale.

IN PLAIN TERMS A Buoy That Must Guess the Next Wave

The main idea. A floating buoy rides up and down on the waves. A generator between the buoy and a post fixed to the seabed turns that motion into electricity. How hard it pushes and pulls decides how much energy it catches.

The challenge. The best push depends on waves that have not arrived yet, so the controller must forecast them from the buoy's own motion. In big seas the generator can push only so hard, and the buoy must never hit the stops at the ends of its travel.

Why it matters. A good forecast of the next few seconds can triple the energy the same buoy brings home.

THREE WAYS TO READ THIS CHAPTER

Explore	11 min	The first page, the fact box of Section 5.1, the history box of Section 5.2, the two try-it boxes, the fact box of Section 5.6, and the key points
Study	45 min	The whole chapter with its pause points and the twelve exercises
Practice	20 min	The first page, Section 5.6, Section 5.7, Section 5.8 and the open challenges

The control question The force that takes the most energy from a wave depends on waves still to come. How much of that anticausal optimum can a controller reach on a forecast built from its own motion, inside a stroke and a force rating that bind in the most energetic seas?

Learning objectives

- Compute the natural period, the intrinsic impedance and the complex-conjugate tuning of a heaving buoy.
- Explain why the optimal velocity draws on the future wave force.
- Describe how a Kalman filter and an autoregressive model estimate and forecast a force no sensor reads.
- Show why the energy-maximizing quadratic program is convex and never credits more than the meter.
- Measure what a forecast horizon is worth, and set a survival threshold for a storm.

Prerequisites Sections 1.4.6 (forecast skill), 1.6.3 (predictive control, Kalman filter) and 1.6.4 (scenarios and data).

The app https://apmonitor.com/apps/wave-energy/

See also Volume 9, Chapter 7 and Volume 9, Chapter 5 for acting on a forecast or ahead of a demand. Volume 5, Chapter 11 and Volume 5, Chapter 13 for estimating what no instrument measures.

5.1 Introduction

In a sea of 1.5 m significant height and 9 s peak period, the simulated buoy, a cylinder 5 m across whose own period is 4.41 s, captures 0.767 kWh in five minutes through a generator set up as a damper tuned to that sea. A model predictive controller (MPC) handed the true wave force over the next 4 s captures 2.713 kWh from the same waves, and 0.862 kWh when it is handed nothing of the future. A forecast that the controller builds from the buoy's own motion brings 2.522 kWh at a 4 s horizon and 1.818 kWh at 1 s. The force that captures the most energy now depends on waves that have not yet reached the buoy.

The objective sets this plant apart from most of the series. A converter is paid for the energy it removes from its disturbance, so its controller optimizes an economic quantity rather than a distance from a setpoint, which is the defining trait of economic model predictive control [1]. The disturbance is also narrowband and partly predictable, so the optimum uses a prediction of it, and any economic controller whose prices or loads come from a forecast has the same shape (Section 1.4.6). The reservoir of Volume 9, Chapter 7 is one, deciding a release days ahead on an ensemble forecast whose error grows with lead time. Reviews of the field treat control as the technology that makes a converter's operation optimal [2], and they survey the optimal, predictive and MPC-like algorithms written for it [3].

✦ DID YOU KNOW? A Coastline's Worth of Waves

The wave energy available along the edge of the United States continental shelf has been estimated at 2640 TWh a year. With arrays packed at 15 MW per kilometer of coastline, 1170 TWh a year of it would be recoverable [4]. The chapter's buoy, tuned as a damper, captures 0.767 kWh in five minutes.

Three beliefs about harvesting waves are contradicted by the cases. The first is that a generator only ever takes power. Tuned as a damper and a spring, the same machine pushes 0.088 kWh back into the sea in five minutes and keeps 1.330 kWh, 1.73 times the damper's, at a peak force of 215 kN against 123 kN. The second is that a controller acts on the wave in front of it. The forecasts above are worth up to 3.1 times the energy of none, because the buoy must already be moving the right way when a crest arrives. The third is that a bigger sea should simply be harvested harder. In a 3.5 m sea a damper tuned for power drives the buoy onto its end-stops twice in five minutes, while the MPC keeps the stroke to 1.22 m and captures 7.011 kWh, and in the graded storm a controller on a real forecast keeps the machine whole only by locking it.

The parts of this problem usually reach a student separately. The hydrodynamic theory of absorption by oscillating bodies [5, 6], the constrained and predictive controllers built on it [3, 7] and short-term wave forecasting [8] live in separate papers, and none of them lets the controllers be run against one sea. This chapter reports, for one declared buoy in a browser simulator, what a damper, reactive control, latching and an energy-maximizing MPC each capture, what force each needs and what forecast each depends on, when all of them act through the same estimate of the wave force. Every method in it is established: the radiation state space [9, 10], the complex-conjugate optimum [6], latching [11] and constrained predictive control of a heaving buoy [7]. The measurements on one buoy and its seeded seas show, among other things, that most of a forecast's value lies within a quarter of the peak period and that the graded storm is passed by a survival lock rather than by harvesting more. The simulator behind them has an eleven-state model whose energy ledger closes to 1.4×10^{-6} through end-stop impacts, a quadratic program made convex by the passivity of the radiation model, a charge for reactive power that is a certified lower bound of the meter, and instruments that are the only route by which any controller learns of the sea. Each of the ten cases is credited by a completion rule of its own.

The chapter is organized as follows. Section 5.2 traces the domain from the first point absorbers to short-term wave forecasting. Section 5.3 states the buoy, the sea, the generator, the meter and the instruments, with every constant. Section 5.4 shows why the force that captures the most must look ahead and why the limits bind in the most energetic seas. Section 5.5 gives the force laws as implemented: the damper, reactive control, latching, the estimate and forecast of the wave force, the energy-maximizing quadratic program and the survival supervisor. Section 5.6 reports the ten cases as measured, the worth of a forecast, the graded storm, what the teaching bound bounds and the verification of the code. Section 5.7 describes the sensors, drives and controllers of real converters, Section 5.8 states the limitations, Section 5.9 summarizes, and the exercises follow in Section 5.10.

5.2 Point Absorbers, Phase Control and Short Forecasts

Modern research on wave energy conversion began in the early 1970s, and the history box at the end of this section tells how its first theory of point absorbers took shape.

The equation of motion that the simulator integrates descends from ship hydrodynamics. A ship-hydrodynamics report of 1962 described ship motions through an impulse response function [12], so that the radiation force becomes an inertia term, the added mass at infinite frequency, plus a convolution of the velocity with a memory kernel. States suit a controller better than a convolution does. A vertical cylinder in heave was given a state-space radiation model in 1995 [9], and identification of such parametric radiation models in the time and the frequency domain was compared for marine structures at zero speed in 2008 [10]. The added mass and damping of a vertical cylinder were computed in 1981 [13], and that matched-eigenfunction approach is the yardstick used in Section 5.6.6

for the simulator's teaching values. The irregular sea uses the spectrum from the measurements of wind-wave growth and swell decay of the Joint North Sea Wave Project (JONSWAP) [14].

Control entered as a question of phase. Latching holds the body still at its turning points, so that a body whose own period is short can keep time with longer waves, and its optimal timing was worked out in regular and irregular waves in 2006 [11]. Limits on motion and force move the optimum into the time domain. A study of a heaving sphere in 2011 optimized the machinery force under such limits, predicted the excitation force with an augmented Kalman filter on a damped harmonic oscillator, and reported a receding-horizon controller that absorbed 90 % or more of the ideal constrained optimum for a chosen range of realistic sea states [7]. Every such controller needs the future of the excitation, as the predictive controller of Chapter 4 needs a preview of the wind. The span of future information that acausal optimal control requires was examined in 2009 [15], short-term wave forecasting for real-time control in 2010 [8], and reviews in 2014 and 2017 set out energy-maximizing control and its predictive algorithms [2, 3]. A generator that loses energy in both directions changes the arithmetic of reactive control, and the effect of a non-ideal power take-off on a reactively controlled converter was quantified in 2014 [16].

> ⧖ HISTORY **From Wave Power to Point Absorbers (1974 to 2002)**
>
> Modern research on wave energy conversion began in the early 1970s, and criteria for the most a converter can absorb soon followed from analysis in the frequency domain [7]. A short paper in *Nature* in 1974 proposed the power of waves at sea as an income to live on, beside solar energy [17]. A second paper, in 1975, called a system a point absorber when its horizontal extent is much smaller than one wavelength: a damped oscillator through which energy passes from the wave to a load [18]. A theory of 1976 gave the efficiency of a damped oscillating body in one or two modes of motion and showed that complete absorption is possible in some cases [5]. A monograph of 2002 gathered the linear theory of waves, oscillating bodies and the absorption of wave energy [6]. Studies of those decades showed that control can raise a converter's absorption by up to 300 % [19].

5.3 The Buoy, the Sea and the Machine

The simulated converter is a vertical cylinder of radius $a = 2.5\,\mathrm{m}$ floating at a draft $d = 4\,\mathrm{m}$ in deep water, free to heave on a spar fixed to the seabed, as shown in Figure 5.1. A linear generator, the power take-off (PTO), has its stator in the spar and its translator carried by the buoy. A brake on the translator serves latching and the survival lock, collars on the spar stop the translator at $\pm x_{max} = \pm 1.5\,\mathrm{m}$ of heave, and a wave probe stands $L = 30\,\mathrm{m}$ upstream. Every number of the buoy, the machine and its limits is a teaching value. A real converter's mass, added mass and damping come from a radiation and diffraction solution for its own hull checked in a wave tank, and its force rating and stroke from the design of its generator and structure and the design sea states of its site. The variables are classified in Table 5.1.

5.3.1 Heave With a Radiation Memory

Linear potential flow gives the heave of a floating body as a balance of the excitation force, the radiation force, the hydrostatic spring and the machine, as shown in Equation (5.1).

$$(m + m_\infty)\,\ddot{x} = f_e(t) - f_r - k_h x - f_{pto} - f_{brk} - f_{end} \tag{5.1}$$

where $m = \rho \pi a^2 d = 80.5\,\mathrm{t}$ is the displaced mass, m_∞ the added mass at infinite frequency, $k_h = \rho g A_{wp} = 197.4\,\mathrm{kN/m}$ the stiffness of the waterplane $A_{wp} = \pi a^2$, f_e the excitation force, f_r the radiation force and f_{pto}, f_{brk} and f_{end} the generator, brake and end-stop forces, positive downward on the buoy. The radiation force is a convolution $\int_0^t K(t-\tau)\dot{x}(\tau)\,d\tau$ in the Cummins form, which the simulator replaces by two states, as shown in Equation (5.2).

$$\dot{z}_1 = z_2, \quad \dot{z}_2 = -a_0 z_1 - a_1 z_2 + \dot{x}, \quad f_r = b_1 z_2 \tag{5.2}$$

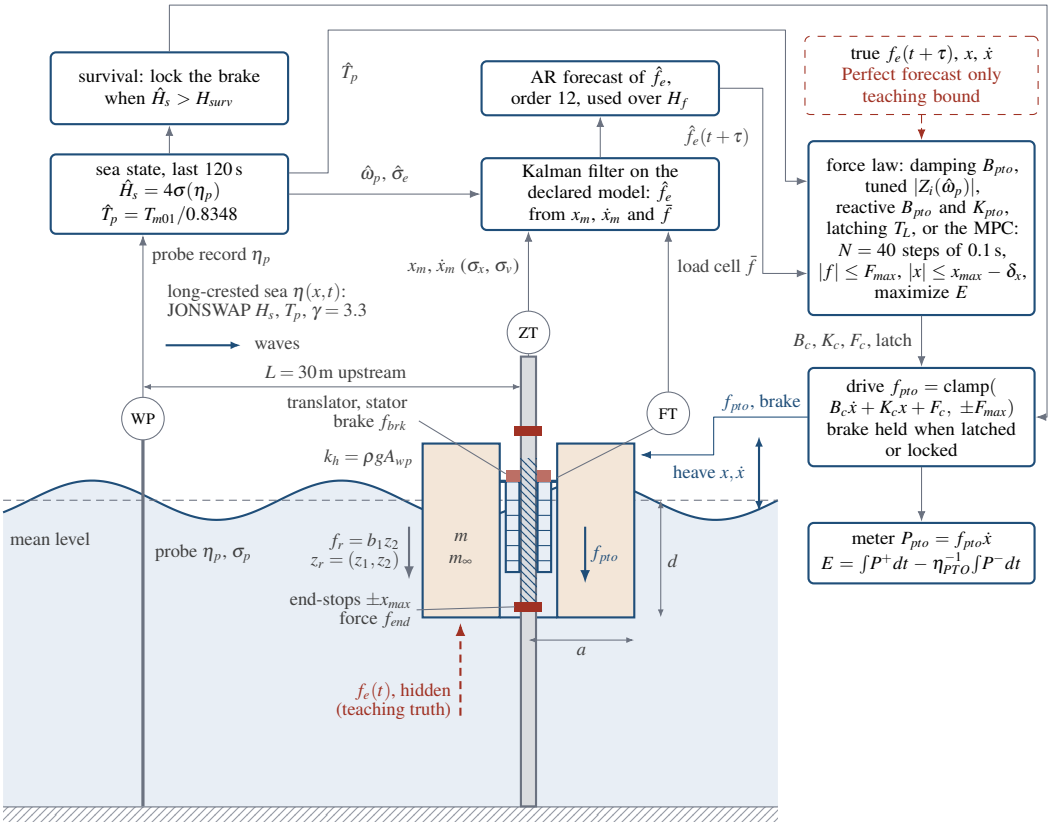


Figure 5.1 The heaving buoy in its sea and in its control loop. The hull is cut through its well to show the spar, the generator's stator and translator, the brake and the end-stop collars. The probe's record feeds the sea-state estimate, the position, velocity and load cell feed the Kalman estimate of the excitation force $\hat{f}_e$, and the true future excitation reaches only the labeled perfect-forecast teaching bound (dashed box and arrow). The estimators sit above the sea, and the force law, the drive and the meter stand beside the buoy.

The transfer function from velocity to force is $\hat{K}(s) = b_1 s/(s^2 + a_1 s + a_0)$, with a zero at the origin, relative degree one and stable poles, the structure a parametric radiation model must keep [10]. Its damping and added mass at frequency ω are given by Equation (5.3).

$$B(\omega) = \operatorname{Re}\hat{K}(i\omega) = \frac{b_1 a_1 \omega^2}{(a_0 - \omega^2)^2 + a_1^2 \omega^2}$$
$$a(\omega) = m_\infty + \operatorname{Im}\hat{K}(i\omega)/\omega \tag{5.3}$$

$B(\omega) \ge 0$ at every frequency because $b_1 a_1 > 0$, so the model is passive, and exactly so in time. The work the buoy does on the water splits into a stored part and a dissipated part, $\int f_r \dot{x}\, dt = \Delta[\frac{1}{2} b_1 (z_2^2 + a_0 z_1^2)] + b_1 a_1 \int z_2^2\, dt$. That identity is what the MPC of Section 5.5 is built on. Both radiation states start at zero, and the buoy starts at rest at $x = 0$ except in case 1, which releases it from $x(0) = 0.5$ m.

5.3.2 A Declared Kernel and Its Two-State Fit

The radiation coefficients are not taken from a boundary-element table. They are fitted to a declared kernel built from the Haskind relation for an axisymmetric body heaving in deep water,

Table 5.1 Variable Classification

Role	Symbol	Meaning	Range or unit
Objective	E	metered energy, maximized	kWh
Constrained	x	heave from rest	$\lvert x\rvert \le 1.5$ m
	f_{pto}	generator force	$\lvert f_{pto}\rvert \le 400$ kN
MV	B_c, K_c, F_c	drive's law and force	per strategy
	brake	latch hold, lock	$T_L \le 6$ s
	F_{man}	force by hand (Manual)	± 400 kN
DV	f_e	excitation force	hidden
	H_s, T_p	sea state	0.1 to 5 m, 4 to 14 s
	events	sea up, rogue group, PTO fault, probe outage	
States	$x, \dot{x}$	heave, velocity	m, m/s
	z_1, z_2	radiation states	m·s, m
	7 integrals	$E^{\pm}$, W_e, E_{rad}, E_{brk}, W_{end}, machine impulse	J, N·s
Measured	$x_m, \dot{x}_m$	encoder, velocity	σ_x, σ_v
	$\bar{f}$	load cell, period mean	exact
	η_p	probe at $-L$	σ_p
Estimated	$\hat{f}_e$	excitation force	kN
	$\hat{H}_s, \hat{T}_p$	sea state from the probe	m, s

$B = \omega k \Gamma^2/(2\rho g^2)$ with $k = \omega^2/g$, applied to the Froude–Krylov force on the flat bottom, which gives the excitation coefficient and the kernel of Equation (5.4).

$$\Gamma(\omega) = \rho g A_{wp}\, e^{-kd}, \qquad B_K(\omega) = \frac{\rho A_{wp}^2}{2g}\, \omega^3 e^{-2d\omega^2/g} \tag{5.4}$$

where Γ is the excitation force per meter of wave amplitude, in phase with the elevation at the buoy. Because B_K and Γ come from one relation, the largest power the model can take from a regular wave, $|\Gamma A|^2/(8B)$, equals the point-absorber limit J/k, the wave power in a crest width of one wavelength over 2π [5, 6, 18]. The three coefficients minimize $\sum_j \ln^2[B(\omega_j)/B_K(\omega_j)]$ on a 0.01 rad/s grid from 0.5 to 2.0 rad/s (wave periods from 3.1 to 12.6 s), which gives $b_1 = 15\,908.67$ N/m, $a_1 = 1.408\,497\,\mathrm{s}^{-1}$ and $a_0 = 1.699\,333\,\mathrm{s}^{-2}$, within 9.8 % of the kernel over the band and 2.8 % rms. The kernel's own initial value $K(0) = (2/\pi)\int B_K\, d\omega$ is 9640 N/m against the model's b_1, so the fit keeps the damping and gives up the shape of the memory at short times. The added mass at infinite frequency is a teaching value, a hemisphere's $\rho\pi a^3/3 = 16.8$ t, not a computed one.

5.3.3 The Sea and the Wave Force

The sea is long-crested and travels toward the buoy along $+x$. Its spectrum is the JONSWAP form with peak enhancement $\gamma = 3.3$, as shown in Equation (5.5).

$$\begin{aligned} S(\omega) &= A_\gamma \tfrac{5}{16} H_s^2 \omega_p^4\, \omega^{-5} \exp\!\big[-\tfrac{5}{4}(\omega_p/\omega)^4\big]\, \gamma^r \\ r &= \exp\!\big[-(\omega-\omega_p)^2/(2\sigma^2\omega_p^2)\big] \end{aligned} \tag{5.5}$$

with $\omega_p = 2\pi/T_p$, $\sigma = 0.07$ below the peak and 0.09 above it, and $A_\gamma = 1 - 0.287 \ln\gamma$. One component is drawn in each of 120 equal bins from 0.30 to 3.00 rad/s, its frequency uniform within the bin and its phase uniform on $[0, 2\pi)$, both from the case's seed, with amplitude $a_k = \sqrt{2S(\omega_k)\Delta\omega}$. The elevation, the excitation and the incident power per meter of crest follow in Equation (5.6).

$$\begin{aligned} \eta(x,t) &= \textstyle\sum_k a_k \cos(\omega_k t - k_k x + \varphi_k) \\ f_e(t) &= \textstyle\sum_k a_k\, \Gamma(\omega_k) \cos(\omega_k t + \varphi_k) \\ J(t) &= \tfrac{1}{2}\rho g \textstyle\sum_k a_k^2\, c_{g,k}, \qquad c_{g,k} = g/(2\omega_k) \end{aligned} \tag{5.6}$$

A change of sea state keeps the frequencies and phases and moves every amplitude linearly to the new spectrum over 60 s. A rogue group adds a narrow-band packet focused on the buoy 30 s after it is fired, with a crest of $1.2H_s$ at ω_p and an envelope of half-width $1.2T_p$, seen first at the probe.

5.3.4 Generator, Brake and End-Stops

Every 0.1 s the controller hands the drive an impedance law and a force, which the drive's own current loop applies continuously, clipped at its rating, as shown in Equation (5.7).

$$\begin{aligned} f_{pto} &= \mathrm{clamp}\big(B_c\dot{x} + K_c x + F_c,\ \pm F_{lim}\big) \\ f_{brk} &= \mathrm{clamp}\big(B_{lt}\dot{x},\ \pm F_{lock}\big) \text{ when engaged} \\ f_{end} &= \mathrm{sgn}(x)\, k_{end}(|x| - x_{max}) + c_{end}\dot{x} \end{aligned} \tag{5.7}$$

where f_{end} acts only while $|x| > x_{max}$, $F_{lim} = F_{max} = 400\,\mathrm{kN}$, halved by a PTO fault, $B_{lt} = 5\,\mathrm{MN\,s/m}$, $F_{lock} = 1.5\,\mathrm{MN}$, $k_{end} = 20\,\mathrm{MN/m}$ and $c_{end} = 570\,\mathrm{kN\,s/m}$. A damper sets B_c, a reactive law B_c and K_c, and the MPC F_c. The brake engages at the first velocity zero crossing after it is armed (and at least 0.2 s after its last release) and releases when its hold is over. Its work heats the brake and is never credited.

5.3.5 The Meter and the Energy Ledger

The meter counts what reaches the grid. Absorbed power $P = f_{pto}\dot{x} > 0$ is credited in full and power pushed back into the sea is charged at $1/\eta_{PTO}$ with $\eta_{PTO} = 0.8$, as shown in Equation (5.8).

$$E = \int_0^t \max(P,0)\,dt - \frac{1}{\eta_{PTO}} \int_0^t \max(-P,0)\,dt \tag{5.8}$$

The capture width ratio divides E by the incident energy across the diameter, $\int J\,2a\,dt$. Seven integrals ride in the state so that the integrator treats them as accurately as the motion: the two parts of the meter $E^{\pm}$, the excitation's work $W_e = \int f_e\dot{x}\,dt$, the radiated energy $E_{rad} = b_1 a_1 \int z_2^2\,dt$, the brake's and the end-stops' work and the impulse of every machine force. They close the ledger $W_e = (E^+ - E^-) + E_{rad} + \Delta E_s + E_{brk} + W_{end}$, with the stored energy $E_s = \frac{1}{2}(m+m_\infty)\dot{x}^2 + \frac{1}{2}k_h x^2 + \frac{1}{2}b_1(z_2^2 + a_0 z_1^2)$.

5.3.6 What the Controllers Measure

The controllers read a packet built once per control period and nothing else, as shown in Equation (5.9).

$$\begin{aligned} x_m &= x + v_x, \qquad \dot{x}_m = \dot{x} + v_v \\ \eta_p &= \eta(-L,t) + v_p \\ \bar{f}_j &= \tfrac{1}{\Delta t}\textstyle\int_{t_{j-1}}^{t_j} (f_{pto} + f_{brk} + f_{end})\,dt \end{aligned} \tag{5.9}$$

where v_x, v_v and v_p are seeded white noise of standard deviation $\sigma_x = 5\,\mathrm{mm}$, $\sigma_v = 0.01\,\mathrm{m/s}$ and $\sigma_p = 0.02\,\mathrm{m}$, and $\bar{f}_j$ is the mean force of a load cell between the buoy and the translator, on which the end-stop collars also act. The packet also carries the rating the drive can deliver and the brake's state. The probe's record of the 120 s before $t = 0$ is handed over at a reset, so the sea-state estimate exists from the start. The excitation force, the elevation at the buoy, the true state and the future are kept from the controllers, exported only in `truth_` columns and drawn dashed on the views. Only the perfect-forecast setting of the MPC adds the true state and the true future excitation to the packet, as a labeled teaching bound.

5.3.7 Constants, Initial State and Integration

Table 5.2 gives every parameter. The engine of Section 1.6.1 integrates Equations (5.1) to (5.8) with fourth-order Runge–Kutta at $h = 10\,\mathrm{ms}$. The stiffest dynamics are the end-stop spring, $\sqrt{k_{end}/(m+m_\infty)} = 14\,\mathrm{rad/s}$ or 44 steps a period, and the engaged brake, $B_{lt}/(m+m_\infty) = 51\,\mathrm{s^{-1}}$ or

Table 5.2 Parameters, Defaults and Their Standing

Symbol	Meaning	Value	Unit, standing
ρ	sea water density	1025	kg/m^3
a, d	radius, draft	2.5, 4.0	m, T
m	mass, $\rho\pi a^2 d$	80.5	t, A
m_∞	added mass, $\omega \to \infty$	16.8	t, T, A
k_h	hydrostatic stiffness	197.4	kN/m, A
b_1	radiation gain	15 908.67	N/m, F, A
a_1	radiation coefficient	1.408497	s^{-1}, F, A
a_0	radiation coefficient	1.699333	s^{-2}, F, A
F_{max}	PTO force rating	400	kN, T, A
x_{max}	end-stops	$\pm$1.5	m, T, A
η_{PTO}	reactive power charge	0.8	T, A
F_{lock}	brake rating	1500	kN, T, A
B_{lt}	brake damping	5000	kN·s/m, T, A
k_{end}	end-stop spring	20	MN/m, H
c_{end}	end-stop damping	570	kN·s/m, H
σ_x, σ_v	encoder noise	5, 0.01	mm, m/s, A
σ_p	probe noise	0.02	m, A
L	probe upstream	30	m, T
γ, N_W	JONSWAP, components	3.3, 120	F
Δt, N	control period, steps	0.1, 40	s
δ_x	MPC stroke margin	0.3	m, C
α	terminal value	0.5	C
p, T_w	AR order, window	12, 60	s, C
H_f	forecast horizon	4	s, C
H_{surv}	survival threshold	0 (off)	m, C

T teaching value, F fitted, A adjustable in the Model dialog, H hidden from the student, C a control on the faceplates. Case settings differ (Table 5.3).

$h\lambda = 0.51$, inside the method's stability region. The controller runs at $\Delta t = 0.1$ s and the historian logs at 10 Hz. Contacts, brake engagements, sea-state changes, the onset of a force cut and the probe's return are events, each processed a single time between two integration steps and marked in the log, and the derivative function reads only the state, the commands the drive holds and the sea's record, so a Reset replays a run bit for bit.

5.3.8 Assumptions

The model assumes linear potential flow in deep water and heave alone, so pitch, surge, viscous drag, moorings and the nonlinear Froude–Krylov force at large motion are absent. These break down for motions comparable to the draft and in steep or breaking seas. The excitation is in phase with the elevation at the buoy, with no diffraction correction. The sea is long-crested and stationary within each state, and its 120 components never repeat within a run. The meter charges only reactive power, so a real generator's losses on absorbed power are missing, and the plant's end-stop is a stiff spring with damping rather than a structural model of an impact.

5.4 Why the Best Force Looks Ahead

5.4.1 A Buoy Tuned to Short Waves

Released from 0.5 m in a 0.2 m sea, the buoy rings at its natural period. The characteristic quartic of Equations (5.1) and (5.2), $(Ms^2 + k_h)(s^2 + a_1 s + a_0) + b_1 s^2 = 0$ with $M = m + m_\infty$, has a dominant pair at $-0.0612 \pm 1.4353i\,\mathrm{s}^{-1}$, a damped period of 4.3777 s against $2\pi\sqrt{M/k_h} = 4.4103$ s, and a damping ratio of 0.043, so each swing is 0.76 of the one before. The seas of the cases have peak periods of 8 to 11 s, about twice the buoy's, and there the intrinsic impedance of Equation (5.10) is

dominated by its reactance.

$$Z_i(\omega) = B(\omega) + iX_i(\omega)$$
$$X_i(\omega) = \omega\big(m + a(\omega)\big) - k_h/\omega \tag{5.10}$$

At 9 s the reactance is −209 kN s/m against a radiation resistance of 4.5 kN s/m, so most of the wave's force goes into accelerating the buoy and the water it carries, not into moving it against a generator.

> **TRY IT IN THE APP** **1 · Free Float: The Natural Period (Start Here)**
>
> Load scenario 1 and press Run. Watch the Heave trend in the first 20 s. The buoy, let go 0.5 m above its rest position, swings at its own period, each swing a little smaller than the one before. The first three swings take 4.38 s each, about half the period of the 8 s waves around it.

5.4.2 The Complex Conjugate and Its Kernel in Time

A linear PTO law $f_{pto} = B_{pto}\dot{x} + K_{pto}x$ in a regular wave of excitation amplitude $F = \Gamma A$ gives the velocity amplitude and mean power of Equation (5.11).

$$\hat{u} = \frac{F}{\left|Z_i + B_{pto} - iK_{pto}/\omega\right|}, \qquad \bar{P} = \tfrac{1}{2}B_{pto}\hat{u}^2 \tag{5.11}$$

A damper alone takes the most at $B_{pto} = |Z_i(\omega)|$. A damper and a spring together take the most at the complex conjugate, $B_{pto} = B(\omega)$ and $K_{pto} = \omega X_i(\omega)$, where the spring cancels the reactance and the power reaches $|F|^2/(8B)$ [6]. Written as an operator on the excitation, the optimum velocity is $\hat{u}_{opt}(\omega) = \hat{F}_e(\omega)/[2B(\omega)]$. Because $1/[2B(\omega)]$ is real and even in ω, its impulse response is even in time, so the optimal velocity at t draws on the excitation at $t + \tau$ as much as at $t - \tau$. The optimum is anticausal, and the question every predictive controller for waves must answer is how much of that future it can see [15]. The reactive spring also costs force. At the tuning of case 3 the peak force rises from 123 kN to 215 kN, and the generator must run as a motor for part of each cycle.

Pause. Try Exercise 5.1 before reading on.

5.4.3 Limits That Bind When the Energy Is Largest

Tuned to the complex conjugate at 9 s, $B_{pto} = 4.5\,\mathrm{kN\,s/m}$ and $K_{pto} = -146\,\mathrm{kN/m}$, the buoy's predicted heave in case 2's 1.5 m sea has three standard deviations of 17.7 m, against a stroke of ±1.5 m. The force rating binds in the same seas, because reactive control's force grows with the motion it creates. Constraints therefore decide the controller in exactly the seas that carry the most energy, and the time-domain problem replaces the frequency-domain optimum [7]. A hit on an end-stop is damage rather than a lost kilowatt-hour, which is why the challenge counts contacts and not only energy.

5.5 The Force Laws as Implemented

The strategies act through Equation (5.7). Free float sets $B_c = K_c = F_c = 0$. Manual mode applies $F_c = F_{man}$ from a hand station, which in Auto follows the force the strategy asks for, so a switch to Manual holds it. Every law designs with the declared model parameters, the plant's own.

5.5.1 Damping, Reactive Tuning and Latching

Damping applies $B_c = B_{pto}$ from its dial. Tuned damping applies $B_c = |Z_i(\hat{\omega}_p)|$ at the probe's estimated peak frequency $\hat{\omega}_p = 2\pi/\hat{T}_p$, re-tuned whenever the estimate moves by a twentieth of a second or of a meter. Reactive control applies B_{pto} and K_{pto} from their dials. Its tuning helper sets $K_{pto} = \hat{\omega}_p X_i(\hat{\omega}_p)$ and the smallest B_{pto} above $B(\hat{\omega}_p)$, rounded to 5 kN/m and 5 kN s/m, for which three standard deviations of the predicted stroke stay inside $0.75\,x_{max}$, with $\sigma_x^2 = \sum_j S(\omega_j)\Delta\omega\,\Gamma^2(\omega_j)/[\omega_j^2|Z_i + B_{pto} - iK_{pto}/\omega_j|^2]$ on 120 frequencies from 0.3 to 3 rad/s, found by bisection. Latching damps at B_{pto}

while the buoy is free and arms the brake with the hold T_L. Its tuning sets $T_L = \max[0, (\hat{T}_{m01} - T_n)/2]$, at most 6 s, from the spectral mean period $\hat{T}_{m01} = 0.8348\,\hat{T}_p$ of a JONSWAP sea with $\gamma = 3.3$ and the natural period $T_n = 2\pi\sqrt{(m+m_\infty)/k_h}$, with $B_{pto} = |Z_i(\hat{\omega}_p)|/2$. In an irregular sea the peak period would hold the buoy too long. On case 4, $T_L = 2.75$ s from $\hat{T}_p$ captures 0.855 kWh against 1.236 kWh with 1.95 s from $\hat{T}_{m01}$.

5.5.2 Estimating and Forecasting a Force No Sensor Reads

The excitation force is what the waves would exert on a buoy held still, and nothing measures it. It is a variable a controller must infer, like the core temperature of the kiln in Volume 5, Chapter 11. A steady-state Kalman filter of the kind described in Section 1.6.3 carries it as a state of a lightly damped resonator beside the buoy's four states, as shown in Equation (5.12).

$$\begin{aligned} \ddot{e} + 2\zeta\hat{\omega}_p\dot{e} + \hat{\omega}_p^2 e = w(t), \qquad q = 4\zeta\hat{\omega}_p^3\hat{\sigma}_e^2 \\ \hat{\sigma}_e = \max\left[20\,\text{kN},\ (\hat{H}_s/4)\,\Gamma(\hat{\omega}_p)\right] \end{aligned} \tag{5.12}$$

with $\zeta = 0.2$ and white noise w of intensity q, so that the stationary variance of e is $\hat{\sigma}_e^2$, the approach of the 2011 heaving-sphere study [7]. The six states $[x, \dot{x}, z_1, z_2, e, \dot{e}]$ evolve by Equations (5.1) and (5.2) with $f_e = e$ and the load cell's $\bar{f}$ as a known input, discretized exactly at 0.1 s together with the process covariance by Van Loan's construction, with a small process noise on the velocity of intensity $[0.02\hat{\sigma}_e/(m+m_\infty)]^2$. The filter measures x_m and $\dot{x}_m$ with $R = \text{diag}(\sigma_x^2, \sigma_v^2)$, and its steady gain is redesigned when $\hat{\omega}_p$ moves by more than 3 % or $\hat{\sigma}_e$ by more than 20 %, at most once every 10 s. Because the end-stop collars act on the translator, the load cell reports their force too, and a contact does not appear to the filter as a burst of wave force.

The sea state comes from the probe's last 120 s. The estimate $\hat{H}_s = 4\sigma(\eta_p)$ follows from the record's variance and $\hat{T}_p = \hat{T}_{m01}/0.8348$ from its spectral mean period $2\pi m_0/m_1$, with the moments summed over a discrete Fourier transform from 0.3 to 3 rad/s at the record's own resolution, every 1 s. While the probe is out, the last estimate holds.

An autoregressive model of order $p = 12$ on samples of $\hat{f}_e$ every 0.5 s, $\hat{e}_k = \sum_{i=1}^{p} \varphi_i \hat{e}_{k-i}$, is fitted by least squares with a ridge of 10^{-6} of the largest diagonal entry to the last 60 s of the estimate, once a second. If the largest root of the fitted polynomial has a modulus $\rho > 0.98$, every coefficient is scaled, $\varphi_i \leftarrow \varphi_i(0.98/\rho)^i$, so an iterated forecast can only decay. The forecast is iterated from the latest p samples, read on the 0.1 s grid by linear interpolation, and set to zero beyond the forecast horizon H_f. Its skill, $1 - \text{MSE}/\overline{\hat{f}_e^2}$ at each lead, is scored against the estimate that later arrives, with a forgetting time of 60 s, which is all the controller itself can check. Section 1.4.6 shows with a first-order model, Equation (1.8), why such a skill falls with the lead.

5.5.3 An Energy-Maximizing Quadratic Program

The MPC chooses the force f_k, held over each 0.1 s step, for $N = 40$ steps (4 s), in 30 move blocks (20 single steps, then pairs). Its model is the plant's heave and radiation, Equations (5.1) and (5.2) without the brake and end-stops, discretized by an exact zero-order hold with the preview w_k of the excitation, the forecast or on the perfect setting the truth at each step's midpoint. The energy the PTO absorbs, $\sum_k f_k \Delta x_k$, is bilinear in force and motion, but the energy balance of the model rewrites it as the excitation's work less the radiated energy and the rise in stored energy. The controller solves the problem of Equation (5.13) every 0.1 s.

$$\begin{aligned} \max_{f,s}\ & \textstyle\sum_k w_k \Delta x_k - b_1 a_1 \Delta t \sum_k c_k z_{2,k}^2 \\ & - c\,\Delta t \textstyle\sum_k \left(f_k - \hat{B}\,\Delta x_k/\Delta t\right)^2 \\ & - (1-\alpha)E_s(N) - \rho_2 s^2 - \rho_1 s \\ \text{s.t. } & |f_k| \le F_{lim}, \quad |x_k| \le x_{max} - \delta_x + s \end{aligned} \tag{5.13}$$

where the sums over the force and the motion run over the N steps, $\Delta x_k = x_{k+1} - x_k$, the slack $s \geq 0$, $c_k = 1$ for $k = 1$ to $N-1$ and $c_N = \frac{1}{2}$ (the trapezoid on the radiated energy), $E_s(N)$ is the stored energy at the horizon's end, valued at the fraction α, and $c = (1/\eta_{PTO} - 1)/(4\hat{B})$ with $\hat{B} = |Z_i(\hat{\omega}_p)|$. Every quadratic weight is non-negative because $b_1 a_1 > 0$ and $\alpha \leq 1$, so the Hessian is positive semidefinite by construction, and the charge on reactive power makes it definite. The charge is a certified lower bound of the meter. For any f, v and $\hat{B} > 0$, $(f - \hat{B}v)^2 + 4\hat{B}fv = (f + \hat{B}v)^2 \geq 0$, so $(f - \hat{B}v)^2/(4\hat{B}) \geq \max(-fv, 0)$, and the objective never exceeds what the meter credits a plan evaluated step by step. The stroke band is soft, with one slack s priced at $\rho_2 = 10^{10}\,\mathrm{J/m^2}$ and $\rho_1 = 10^8\,\mathrm{J/m}$, far above any energy on offer, and the force bound is hard at the rating the drive reports. The quadratic program is solved by the framework's condensed linear MPC on its dense dual active-set solver (Section 1.6.3), capped at 300 iterations. A failed solve falls back to the passive optimum $\hat{B}$ for that period and is counted on the faceplate.

🕮 **Pause.** Try Exercise 5.3 before reading on.

5.5.4 Survival, the Teaching Bound and Three Models

The survival supervisor works on the probe's estimate alone. When $\hat{H}_s$ exceeds H_{surv}, the brake locks the buoy at its next velocity zero crossing while the strategy keeps control until the brake holds, after which the PTO idles. It unlocks when $\hat{H}_s$ has stayed 0.5 m below the threshold for 60 s, and a contact during survival stops the run. The perfect-forecast teaching bound of each case is the MPC of Equation (5.13) on the true state and the true future, at $H_f = N\Delta t = 4\,\mathrm{s}$, a margin of 0.01 m and $\alpha = 1$, with no survival lock. Three models are kept apart. The plant is the whole of Section 5.3. The filter and the MPC carry the plant's declared heave and radiation, with the excitation a resonator in one and a forecast preview in the other. The tunings use the frequency-domain impedance of Equation (5.10) at one estimated frequency.

5.6 Ten Cases on One Buoy

The ten cases are listed in Table 5.3. Every number below was measured on the app's own engine, headless, at the case's seed (20261030, and 3 for the challenge), over the case's own run, with the settings named entered before Run. The measured outcomes are collected in Table 5.4, and Figure 5.2 draws them as a chart. Each case carries a briefing and a completion rule (Section 1.6.4), and the rule credits the decision the case asks for rather than a state the plant happens to reach. Case 5, for example, is earned by finishing a run with the perfect forecast at a horizon of 0.5 s or less, then setting it to 3 s or more and capturing at least 2.0 kWh in a second run. A scripted walk earns every rule, and a run on the shipped settings earns none.

5.6.1 Resonance, Damping and a Two-Way Machine

Case 1 releases the buoy 0.5 m up in a 0.2 m sea at 8 s. Its first three swings take 4.38 s each, within 1 % of the 4.41 s formula. Over 120 to 180 s the heave's rms is 1.5 times the sea's at 8 s and 2.37 times with the peak period set to 4.5 s, near resonance. In case 2's 9 s sea the shipped damper of 40 kN s/m captures 0.474 kWh in five minutes (5.7 kW, a capture width ratio of 13 %). Tuned to the sea, 215 kN s/m, it captures 0.767 kWh (9.2 kW, 21 %), and swept by hand the best damping, 175 kN s/m, captures 0.785 kWh, so the optimum is flat. The tuned damper resists hard and lets the buoy move less, from 1.31 m to 0.79 m of stroke, and its velocity runs about 0.7 s ahead of the excitation. Reactive control in case 3, $K_{pto} = -145\,\mathrm{kN/m}$ and $B_{pto} = 210\,\mathrm{kN\,s/m}$, captures 1.330 kWh while the power dips to −22.8 kW in the worst wave. Latching in case 4's 10 s sea captures 1.236 kWh against the tuned damper's 0.747 kWh, with the buoy held 43 % of the time. A controller that spends almost half of each wave doing nothing captures 1.65 times as much, because the buoy then moves while the wave force is with it.

🕮 **Pause.** Try Exercise 5.2 before reading on.

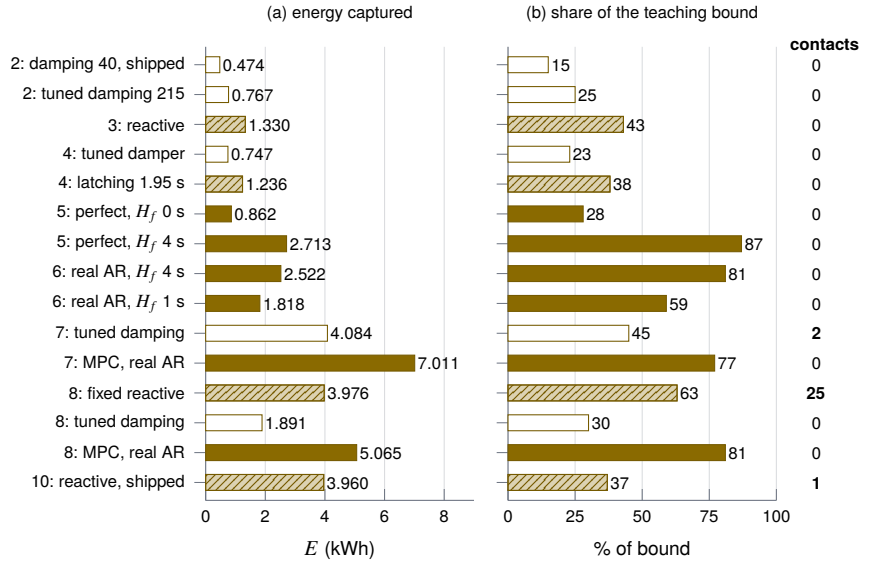


Figure 5.2 Table 5.4 as a chart: (a) the energy each controller captured and (b) its share of the case's perfect-forecast teaching bound, with the end-stop contacts of each run at the right. White bars are damping, hatched bars reactive control and latching, solid bars the MPC. Notice that in cases 7 and 8 the MPC captures the most and touches no stop, while the fixed reactive law of case 8 comes second while striking the stops 25 times.

Table 5.3 Scenarios

Case	Sea H_s, T_p	Shipped settings and lesson	Run
1	0.2 m, 8 s	free float from 0.5 m, natural period	180 s
2	1.5 m, 9 s	damping 40 kN·s/m, tune to the sea	300 s
3	1.5 m, 9 s	tuned damper, then reactive	300 s
4	1.5 m, 10 s	tuned damper, then latching	300 s
5	1.5 m, 9 s	MPC, Perfect forecast, H_f 0 s	300 s
6	1.5 m, 9 s	MPC, Real AR forecast, H_f 4 s	300 s
7	3.5 m, 9 s	tuned damping, then MPC	300 s
8	1.5 m, 8 s	reactive B 165, K −135, then 2.5 m, 11 s from 120 s	420 s
9	three seas	challenge: damping 170 kN·s/m	1200 s
10	4.0 m, 10 s	reactive B 630, K −155 (infeasible)	300 s

B in kN·s/m, K in kN/m. The challenge's seas are 1.5 m at 8 s, 2.5 m at 9 s from 340 s and 4 m at 10 s from 740 s.

5.6.2 What a Forecast Is Worth

Cases 5 and 6 run the MPC in the same 9 s sea, with the true future and with the autoregressive forecast of the controller's own estimate, as shown in Figure 5.3. With no forecast the plan always ends with the buoy at rest, and the MPC captures 0.862 kWh, 12 % more than the tuned damper's 0.767 kWh. A perfect forecast adds energy at every horizon: 1.790 kWh at 0.5 s, 1.847 at 1 s, 2.213 at 1.5 s, 2.500 at 2 s, 2.673 at 3 s and 2.713 at 4 s, with a peak force of 294 kN and 0.509 kWh pushed back into the sea. The real forecast tracks it closely up to 1 s (1.818 against 1.847 kWh) and falls behind as the lead grows, to 2.522 against 2.713 kWh at 4 s, 93 % of the perfect forecast's energy.

Table 5.4 Measured Results of Cases 2 to 8 and 10

Case	Controller	E (kWh)	Bound	Peak (kN)	Contacts
2	damping 40, shipped	0.474	15 %	44	0
2	tuned damping 215	0.767	25 %	123	0
3	reactive K −145, B 210	1.330	43 %	215	0
4	tuned damper	0.747	23 %	136	0
4	latching 1.95 s, B 120	1.236	38 %	166	0
5	Perfect, H_f 0 s	0.862	28 %	138	0
5	Perfect, H_f 4 s	2.713	87 %	294	0
6	Real AR, H_f 4 s	2.522	81 %	312	0
6	Real AR, H_f 1 s	1.818	59 %	237	0
7	tuned damping	4.084	45 %	291	2
7	MPC, Real AR	7.011	77 %	400	0
8	fixed reactive	3.976	63 %	313	25
8	tuned damping	1.891	30 %	238	0
8	MPC, Real AR	5.065	81 %	400	0
10	reactive, shipped	3.960	37 %	400[a]	1

Bound: the share of the case's perfect-forecast teaching bound (3.1032 kWh on cases 2, 3, 5 and 6, 3.2601 on case 4, 9.0726 on case 7, 6.2665 on case 8, 10.7592 on case 10). Peak: the largest force applied. [a] asked 897 kN before the rating cut it.

The forecast's own skill explains the gap. Averaged uniformly over 237 forecasts made every second from 60 to 296 s, it is 0.96, 0.85, 0.82 and 0.78 at leads of 1, 2, 3 and 4 s against the estimate that later arrived, and 0.95, 0.85, 0.83 and 0.78 against the true excitation, so the skill the controller can check is the skill it has. The forecast's worth arrives early. Half of the gain from no forecast to a 4 s perfect forecast comes from the first 0.5 s, and 88.5 % of it from the first 2 s, less than a quarter of the 9 s peak period.

> **TRY IT IN THE APP** **5 · The Anticausal Optimum: A Perfect Forecast Against None**
>
> Load scenario 5 and run the five minutes. The predictive controller has a perfect forecast but a Forecast horizon of 0 s, and it captures 0.862 kWh. Set the Forecast horizon to 4 s, press Reset and run again. The same waves now give 2.713 kWh, and the peak force rises from 138 kN to 294 kN.

The estimate behind the forecast is accurate. Sampled at the control instants after the first 30 s, its error is 6.0 % rms of the true force on case 6 and 4.0 % on case 7 under the MPC. After an end-stop contact, the largest error within 3 s is 40.0 kN on case 7's tuned damper and at most 51.6 kN in the challenge, because the load cell reports the collar's force.

5.6.3 Strokes, Ratings and Changing Seas

In case 7's 3.5 m sea the tuned damper reaches 1.54 m of stroke and hits the end-stops twice for 4.084 kWh. The MPC on the real forecast keeps the stroke to 1.22 m with no contact, at its 400 kN rating, and captures 7.011 kWh, and on the perfect forecast 7.506 kWh. A damper can only resist a motion that is already there, while the MPC sees the big wave in its forecast and starts braking the swing before it. Its plan carried slack three times, for 1.6 s in all, when even the full rating could not hold the plan 0.3 m inside the stops, and the margin absorbed it. In case 8 the sea grows from 1.5 m at 8 s to 2.5 m at 11 s at 120 s. The reactive settings tuned for the first sea hit the stops 25 times from 198 s on. Tuned damping follows the probe's estimate of the peak period, from 8.3 s at 120 s to 11.5 s at 300 s, raising its damping from 182 to 305 kN s/m, and never touches a stop, for 1.891 kWh. The MPC captures 5.065 kWh with no contact. With the probe out from 60 s, the estimate holds at 8.1 s at 240 s and the tuned damper still captures 1.869 kWh, because a passive damper is forgiving where a reactive tuning is not.

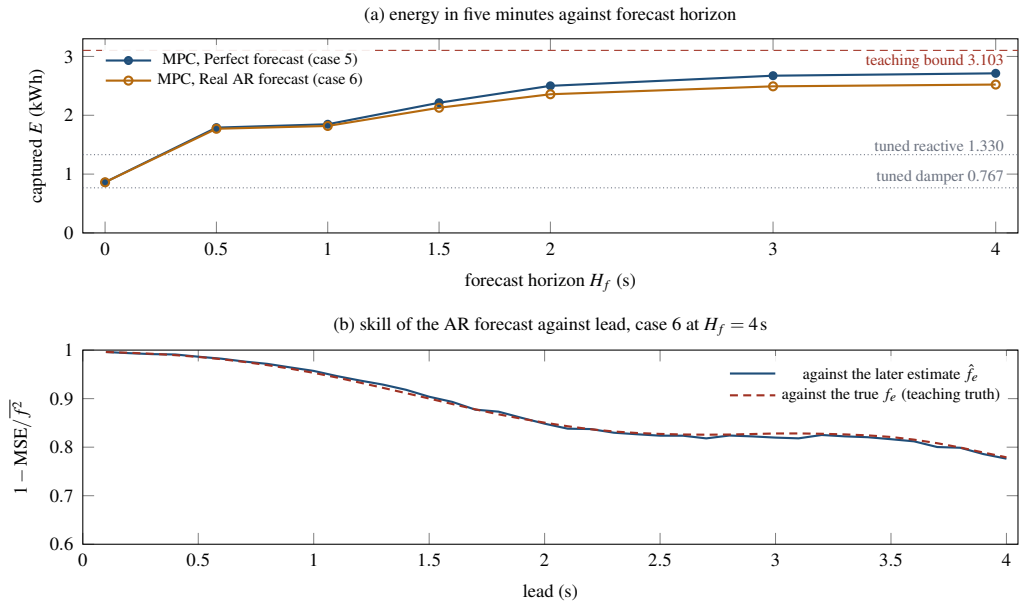


Figure 5.3 The worth of a forecast in the 1.5 m, 9 s sea of cases 5 and 6. (a) Energy captured in five minutes against the forecast horizon on the perfect forecast (solid line, filled circles) and on the real forecast (solid line, open circles), beside the tuned damper and tuned reactive control (dotted lines) and the case's teaching bound (dashed line). (b) The AR forecast's skill against lead, scored against the later estimate (solid line) and against the true excitation (dashed line).

Case 10 is the deliberately infeasible variant. Reactive control tuned for its 4 m, 10 s sea, $K_{pto} = -155\,\mathrm{kN/m}$ and $B_{pto} = 630\,\mathrm{kN\,s/m}$, asks the drive for 897 kN and still touches a stop once. Swept from 100 to 1000 kN s/m at that stiffness, the asked force runs from 395 kN with 132 contacts to 1007 kN with none, so every damping breaks one limit or the other, as does every softening stiffness with damping alone. The claim is scoped to the softening, reactive tuning. A stiffening spring of +50 kN/m or more, which detunes the buoy from these waves, keeps a linear law inside both limits at 3.8 kWh at best, and the MPC keeps both by planning its force, at 8.33 kWh on the real forecast.

> **+ DID YOU KNOW? More Energy and Fewer Hits**
>
> From the simulator: in the 3.5 m sea of case 7, the tuned damper captured 4.084 kWh and struck the end-stops twice. The predictive controller on its own forecast captured 7.011 kWh with no contact (Table 5.4). The controller that took more energy was also the one that spared the stops.

5.6.4 Twenty Minutes Through a Storm

The challenge runs one recorded sea, the same on every run, through 1.5 m, 2.5 m and a 4 m storm. It passes at 9.33 kWh or more, 40 % of the case's teaching bound of 23.3248 kWh, with no end-stop contact and no force asked of the drive beyond 400 kN, on the real forecast, as shown in Table 5.5. The shipped damper fails on contacts and energy. The MPC without survival captures 18.585 kWh, 79.7 % of the bound, but hits the stops twice in the storm. With the threshold at 3.3 m, the probe's $\hat{H}_s$ of 3.37 m trips the supervisor at 872.0 s, the brake engages at the buoy's next turning point at 872.4 s and holds it for the last 328 s, and the run keeps the 2.606 kWh and 5.927 kWh harvested in the first two seas. While locked, the brake carries at most 703 kN of its 1500 kN against an excitation of at most 537 kN, and the buoy creeps at no more than 0.141 m/s within 1.223 m. The state at 873.0 s is shown in Figure 5.4. Every threshold from 3.2 to 3.5 m passes, 3.0 and 3.1 m lock in the 2.5 m sea,

Table 5.5 The Challenge on Its Recorded Sea (Seed 3)

Policy	E (kWh)	Bound	Contacts	Verdict
shipped damping 170	8.909	38.2 %	23	fail
MPC real, no survival	18.585	79.7 %	2	fail
MPC real, H_{surv} 3.0 m	8.022	34.4 %	0	fail
MPC real, H_{surv} 3.3 m	**10.889**	**46.7 %**	**0**	**pass**
MPC real, H_{surv} 3.6 m	11.171	47.9 %	1	fail
tuned damping, H_{surv} 3.3 m	4.472	19.2 %	3	fail
perfect bound (teaching)	23.325	100 %	0	not graded

On six seeds the suggested setting (bold) never touches a stop and reaches 40 % of each seed's own bound on four (51.5, 46.9, 46.7 and 43.4 %, against 38.1 and 37.8 % on seeds 5 and 6). The MPC without survival touches the stops on seeds 3 and 5.

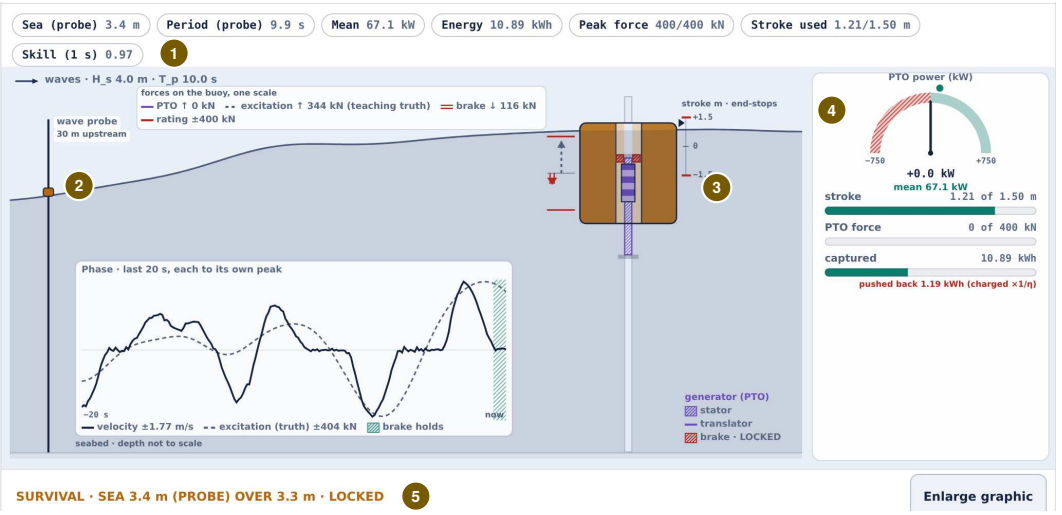


Figure 5.4 The challenge with the suggested settings (MPC on the real forecast, horizon 4 s, survival threshold 3.3 m) at $t = 873.0$ s, cropped to the Sea view. The probe reads 3.4 m and 9.9 s in the 4 m, 10 s storm, the brake has held the buoy at 1.21 m of heave since 872.4 s, and the generator applies 0 kN while the brake carries 116 kN against an excitation of 344 kN (teaching truth). The meter reads 10.89 kWh, and 1.19 kWh has been pushed back into the sea and charged at $1/\eta_{PTO}$. Callouts: (1) the badge row with the probe's sea state, (2) the wave probe upstream, (3) the buoy held by its brake on the spar, (4) the PTO power meter with the stroke, force and energy bars, and (5) the status line of the survival lock.

where $\hat{H}_s$ reaches 3.11 m, and 3.6 m touches a stop while locking. The lock costs 7.7 kWh against the MPC without survival, the price of not seeing the storm's biggest group coming.

The verdict belongs to one sea. On six seeds, each against its own bound, the shipped damper captures 37.4 to 39.3 % with 11 to 39 contacts every time, the MPC without survival rides out four storms and touches the stops on two, and the suggested setting stays off the stops on all six while reaching the target on four. A controller cannot know which sea it will meet, so the lock is insurance. The force term of the target never decides a verdict. Among nine student-like policies with survival and the 597 graded challenge runs of the search below, every one that asked for more than 400 kN also hit the stops or fell short of the energy, so the term states the rating and catches a law that leans on the drive's cut. A run that used the perfect forecast for even 1 s is not graded.

5.6.5 What the Bound Bounds

Each case's bound is the MPC of Equation (5.13) on the true future, planning to within 0.01 m of the stops where the student's controllers keep 0.3 m, and valuing the energy still stored at the horizon's end in full. A search of 6620 runs over every strategy and every setting a student can reach, 662 on each case, from damping and reactive laws over their whole dial ranges to latching, the MPC's horizon, margin, terminal value and the AR order and window on both forecasts, found none above it. The best perfect-forecast setting a student can reach (margin 0.05 m, $\alpha = 1$) comes to 97.6 to 98.5 % of it on cases 2 to 10, and ties it in case 1's small sea, where no margin binds. The best real forecast comes to 91.2 to 94.3 %. The word bound is scoped to what the app offers. It is not the most a buoy could capture. A plan solved offline over 60 s windows on the same discrete model, with the whole window's excitation known, stays within −0.51 to +0.22 % of the receding 4 s MPC over the first 50 s of each window, and gains 0.9 to 6.7 % only at the window's end by spending the energy stored in the buoy. The certified charge on reactive power is conservative. On case 6's sea, the perfect-forecast MPC at the bound's settings captures 3.1032 kWh with the certified charge and 3.3534 kWh with half of it, 8 % more, though the halved charge is no longer a lower bound of the meter. Every MPC in the app and its bound pay the same charge, so no comparison among them is unfair.

5.6.6 Code Verification and Agreement With Published Theory

Code verification tests the program against closed-form results and against the conservation laws it should obey. The hydrostatics computed by hand equal the source to the last digit printed. The free decay's period of 4.3777 s from the characteristic quartic matches the 4.38 s swings of the simulated decay, and the storage identity of the radiation model holds on a random velocity to 3.5×10^{-8} relative. In a regular wave at the model's resonance (4.3795 s, $A = 0.25$ m, $B_{pto} = B(\omega_0)$), the time-domain capture over 40 whole periods equals $|F|^2/(8B)$, 5.1911 kW, to 10^{-5}, and off resonance at 8 and 10 s the time and frequency domains agree to four digits. The energy ledger closes to 1.44×10^{-6} of the excitation's work over 900 s of the challenge with eight end-stop impacts, to 7.9×10^{-9} with the survival lock, to 9.2×10^{-8} under latching and to 4.4×10^{-8} with the force cut in case 10. Halving the step to 5 ms moves the challenge's energy by at most 0.0016 % with the same contacts. In the MPC, the balance form of the objective agrees with the exact $\sum f_k \Delta x_k$ to 0.0138 % on 200 random force sequences. The Hessian's smallest eigenvalue, with force in newtons and the app's 30 blocks, is 4.2×10^{-13} for the exact bilinear form, 2.1×10^{-14} for the balance form and 6.0×10^{-8} with the charge. The plant's continuous meter differs from the plan's step meter by at most 0.077 % of a run. At every one of 312 plans that carried slack, a feasibility linear program on the same state, preview, rating and blocks found that no force within the rating could avoid it, so the penalty is exact. In Node a solve takes 0.267 to 0.290 ms on average, 3.65 ms at most, with no failure. In Chrome at 30 times real time the challenge's twenty minutes take 40.0 s of wall time, with mean solves of 0.287 and 0.313 ms for the suggested setting and the bound and 6.30 ms at most.

Agreement with published theory is a separate matter, and here the model departs from the hull it draws. A matched-eigenfunction solution of this cylinder, the method of [13], gives an added mass at infinite frequency of 30.4 t against the teaching 16.8 t and a natural period of 4.67 s against 4.38 s. Against it the teaching model sits 28 to 31 % low on the added mass over 0.4 to 1 rad/s, and 14 to 27 % high on the radiation damping and 3 to 14 % high on the excitation over 0.4 to 0.8 rad/s. The lessons rest on the model's own consistency, its point-absorber limit, its passivity and its ledger, and not on these values. The JONSWAP form of Equation (5.5) integrates to $4\sqrt{m_0} = 1.0012 H_s$ and a ratio T_{m01}/T_p of 0.8344 against the 0.8348 the estimator uses. The probe leads the buoy by 2.55 s at the peak of the elevation's cross-correlation in the 9 s sea, between the deep-water phase delay of 2.13 s and group delay of 4.27 s. At 120 s the probe's $\hat{H}_s$ falls within 4.6 % of the sea as set and $\hat{T}_p$ within 3.9 % on four seas. The app has had no educational evaluation.

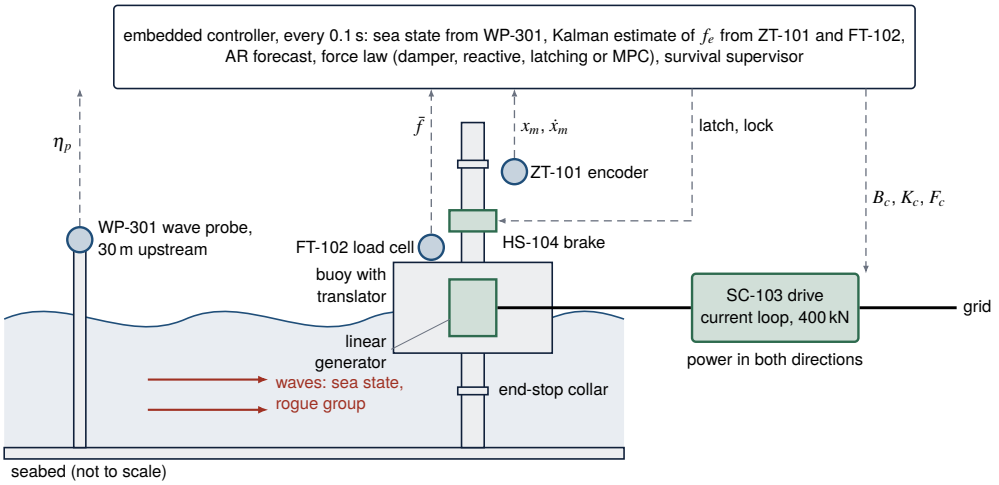


Figure 5.5 The force loop drawn with its hardware. The wave probe WP-301 reads the sea 30 m upstream, the encoder ZT-101 reads the heave and its velocity, and the load cell FT-102 reads the mean force between buoy and translator, collars included. The embedded controller turns them into a force law every 0.1 s, the drive SC-103 applies it continuously through the linear generator within 400 kN, and the brake HS-104 holds the buoy for latching and the survival lock. Notice that no instrument reads the wave force f_e that the optimum needs: the controller estimates it.

5.7 Technology in Practice

The force laws of Section 5.5 read three instruments and move two final elements, the drive of the linear generator and the brake. Figure 5.5 draws the loop with that hardware in place of the schematic's symbols.

What Measures It

The heave and its velocity come from a position sensor between buoy and spar. An encoder reads a position directly, and a speed is derived from the change of position with time [20]. The force comes from a load cell, strain gauges bonded to a metal element that stretches and compresses with the applied force as though it were an extremely stiff spring [21]. Stray electric currents through a load cell are read as changes of force [21]. The sea is read upstream, at sea by a measurement buoy. The chapter's encoder carries 5 mm and 0.01 m/s of noise, and its load cell reports the exact mean force of each period with the collars' force included, which is why an end-stop contact does not look like a burst of wave force to the filter.

> **TECHNOLOGY Sensor: A Wave Buoy That Feels the Sea**
>
> A wave buoy measures the sea through its own motion. An accelerometer with its axis perpendicular to the deck records the vertical acceleration, and the acceleration spectrum becomes a displacement spectrum when it is divided by the fourth power of the radian frequency. One buoy system analyzes 20 min records sampled at 1.5 Hz, and the significant wave height comes from the variance of the elevation, with 90 % confidence limits of about −10 % and +15 % [22]. The division amplifies electronic noise at low frequency, so a poorly corrected record shows low-frequency swell that is not real [22]. The chapter's probe reports the elevation every control period with 0.02 m of noise, and its sea-state estimate uses the last 120 s.

What Moves It

A power electronic converter sets the generator's current and so its force. A power take-off that pushes as well as pulls must pass power in both directions, a capability that many published designs

neglect [23]. The chapter's drive follows its law continuously between control instants, clipped at its 400 kN rating and at half of it after a fault. The brake is the second final element. It clamps the translator for latching and for the survival lock, with a rating of 1.5 MN, and its work is never credited.

> **TECHNOLOGY** **Final Element: A Direct-Drive Linear Generator**
>
> Waves deliver their energy at large forces and low velocities. Hydraulics or turbines can turn the slow motion into fast rotation, and a direct-drive linear generator takes it with fewer moving parts [24]. In one sea-trial converter a translator carrying permanent magnets moves inside the stator windings, end stops limit its stroke in the most powerful seas, and the generator is rated 10 kW at 0.67 m/s with 1.8 m of free stroke. Its voltage varies in amplitude and frequency, so its current is rectified and inverted again before it reaches the grid. A contact with an end stop shows on a trend as a sharp peak in the measured line force [24]. The chapter's drive applies its force law through a current loop clipped at 400 kN.

Where the Controller Runs

On a test device the most common arrangement is an integrated one: a dedicated controller packaged with the sampling hardware and embedded in the device, which acquires, scales and checks the measurements and also performs the control logic [20]. Supervisory and lower-level control loops run with cycle times from milliseconds to minutes [25]. The chapter's controller runs every 0.1 s and solves its quadratic program in at most 3.65 ms in Node. A practical controller often stores one set of gains for each bin of significant wave height and period and updates them when the sea changes, every several minutes [19], much as the tuned damper of this chapter re-tunes from the probe's estimate.

> **IN PRACTICE** **Check the Data Before the Power**
>
> The power performance of a wave energy converter is assessed against the technical specification IEC TS 62600-100, and accredited testing to it adds requirements and cost to sensor selection and data acquisition [20]. Each sensor carries its own calibration, because two identical load cells can read 3.10 V and 3.15 V under the same reference weight. In service, automated checks run in near real time: a value outside its expected range, a change too large or no change at all between samples, and a lost correlation between two signals that should agree, such as generator shaft speed and generator voltage [20].

What Is Modernizing It

Three developments touch this loop. Control co-design sizes the power take-off and its controller together, because a device designed for the most mechanical power may carry a needlessly costly specification [19]. All-electric power take-offs built on modular multilevel converters have been tested with controllers on field programmable gate arrays, although marine energy remains at an early stage of technology readiness without a commercial breakthrough [23]. Learning-based controllers have adjusted the damping of a marine current turbine as marine growth changed it, without measuring the growth [26], a remedy for the model drift that the estimator and the MPC of this chapter do not face.

5.8 Limitations

The hydrodynamics are a teaching model. The kernel is declared, the two-state fit is within 9.8 % of it, and against the cylinder's own coefficients the added mass is about 30 % low and the damping and excitation up to 27 % and 14 % high over the band of interest, so the natural period is 4.38 s where the hull would ring at 4.67 s. Numbers for a real buoy would move, while the ranking of the controllers rests on the model's own consistency. The estimator and the MPC use the plant's exact model, so model error, which a real controller's margin would also have to cover, is absent. The sea has 120 components, and the challenge's record shows a normalized autocorrelation of 0.49 at a lag of 478 s, so its wave groups resemble each other more than a real record's. The probe's peak period is within 4 %, not exact, and the latch rule inherits that error.

OPEN CHALLENGE **Marine Growth Moves the Optimum**

In simulations of a reference point absorber in a 2 m sea at its resonant 12 s period, heavy marine growth on the hull cut the power by 15 %, and re-tuning the damping recovered only about 6 % of the loss. A failure study of a 100 kW reference converter ranked marine growth, with up to 45 % less power, and power take-off failures among the costliest risks [26]. The chapter's hull never changes. Progress would be adaptive controllers and models that follow a hull as it degrades in service [26].

The reactive charge is a certified lower bound of the step meter, which the plant's continuous meter matches within 0.08 %, and it costs about 8 % of the perfect forecast's energy on case 6's sea. The shipped terminal value $\alpha = 0.5$ is not the best setting. At the shipped margin, $\alpha = 1$ changes the energy by -0.02 to $+0.48$ % on cases 2 to 10 and by 1.5 to 1.6 % in case 1. The challenge's verdict belongs to one recorded sea, and the suggested setting misses the target on two of six seeds. The 400 kN term of the target never binds alone. The force rating, the stroke, the brake, the efficiency and the survival threshold are teaching values, and passing the challenge in simulation certifies no converter and checks no design.

OPEN CHALLENGE **Optimal Control on a Real Machine**

Two issues limit the classical theory of complex-conjugate control on a real converter: the optimum is noncausal, and the interaction of body and water and the power take-off itself are nonlinear [19]. The excitation force cannot be measured directly, and a controller that maximizes mechanical power may absorb a net negative amount of electricity once the losses of the power take-off are counted [19]. The chapter's controllers use the plant's exact model and a meter that charges only reactive power, so neither problem appears in full. Progress would be controllers designed together with the machine and judged by the electricity they deliver.

5.9 Conclusion

A heaving buoy whose own period is half the waves' captures little through a damper and much more through a controller that knows the coming wave force, and this chapter has measured that difference on one declared model. The tuned damper takes 0.767 kWh in five minutes, reactive control 1.330 kWh at nearly twice the peak force, latching 1.236 kWh in a longer sea, and the MPC 2.713 kWh on a perfect 4 s forecast and 2.522 kWh on a forecast built from its own Kalman estimate. In a 3.5 m sea the MPC keeps the stroke to 1.22 m where a tuned damper hits the stops, and in the twenty-minute storm a survival lock on the probe's estimate passes the target at 10.889 kWh with no contact. The hydrodynamics are a teaching kernel that departs from the real cylinder's by up to 31 %. A fuller model would add pitch and surge, a hull computed by a boundary-element method, model error in the controller, a generator that loses energy both ways, and an array of buoys sharing one sea. The buoy makes anticausal optimal control something a reader can run, measure and break.

KEY POINTS

- A heaving buoy turns wave motion into electricity through a generator whose force a controller sets, and the force that captures the most depends on waves still to come.
- The tuned damper takes 0.767 kWh in five minutes, reactive control 1.330 kWh, and the MPC 2.713 kWh on a perfect 4 s forecast and 2.522 kWh on its own forecast.
- Most of a forecast's value lies within a quarter of the peak period.
- In a 3.5 m sea the MPC keeps the stroke to 1.22 m where a tuned damper hits the stops, and the graded storm is passed by a survival lock rather than by harvesting more.

Where else this applies. An economic controller acting on a forecast also decides the reservoir release of Volume 9, Chapter 7, and a preview of the disturbance feeds the predictive controller of Chapter 4.

References

[1] M. Ellis, H. Durand, and P. D. Christofides, "A tutorial review of economic model predictive control methods," *Journal of Process Control*, vol. 24, no. 8, pp. 1156–1178, 2014.

[2] J. V. Ringwood, G. Bacelli, and F. Fusco, "Energy-maximizing control of wave-energy converters: The development of control system technology to optimize their operation," *IEEE Control Systems*, vol. 34, no. 5, pp. 30–55, 2014.

[3] N. Faedo, S. Olaya, and J. V. Ringwood, "Optimal control, MPC and MPC-like algorithms for wave energy systems: An overview," *IFAC Journal of Systems and Control*, vol. 1, pp. 37–56, 2017.

[4] G. Hagerman, G. Scott, and P. Jacobson, "Mapping and assessment of the United States ocean wave energy resource," Electric Power Research Institute, Palo Alto, CA, Tech. Rep. 1024637, 2011.

[5] D. V. Evans, "A theory for wave-power absorption by oscillating bodies," *Journal of Fluid Mechanics*, vol. 77, no. 1, pp. 1–25, 1976.

[6] J. Falnes, *Ocean Waves and Oscillating Systems: Linear Interactions Including Wave-Energy Extraction*. Cambridge University Press, 2002.

[7] J. Hals, J. Falnes, and T. Moan, "Constrained optimal control of a heaving buoy wave-energy converter," *Journal of Offshore Mechanics and Arctic Engineering*, vol. 133, no. 1, p. 011401, 2011.

[8] F. Fusco and J. V. Ringwood, "Short-term wave forecasting for real-time control of wave energy converters," *IEEE Transactions on Sustainable Energy*, vol. 1, no. 2, pp. 99–106, 2010.

[9] Z. Yu and J. Falnes, "State-space modelling of a vertical cylinder in heave," *Applied Ocean Research*, vol. 17, no. 5, pp. 265–275, 1995.

[10] T. Perez and T. I. Fossen, "Time- vs. frequency-domain identification of parametric radiation force models for marine structures at zero speed," *Modeling, Identification and Control*, vol. 29, no. 1, pp. 1–19, 2008.

[11] A. Babarit and A. H. Clément, "Optimal latching control of a wave energy device in regular and irregular waves," *Applied Ocean Research*, vol. 28, no. 2, pp. 77–91, 2006.

[12] W. E. Cummins, "The impulse response function and ship motions," David Taylor Model Basin, Report 1661, Oct. 1962.

[13] R. W. Yeung, "Added mass and damping of a vertical cylinder in finite-depth waters," *Applied Ocean Research*, vol. 3, no. 3, pp. 119–133, 1981.

[14] K. Hasselmann *et al.*, "Measurements of wind-wave growth and swell decay during the Joint North Sea Wave Project (JONSWAP)," *Ergänzung zur Deutschen Hydrographischen Zeitschrift, Reihe A (8)*, no. 12, pp. 1–95, 1973.

[15] A. A. E. Price, D. I. M. Forehand, and A. R. Wallace, "Time-span of future information necessary for theoretical acausal optimal control of wave energy converters," in *2009 European Control Conference (ECC)*, 2009, pp. 3761–3766.

[16] R. Genest, F. Bonnefoy, A. H. Clément, and A. Babarit, "Effect of non-ideal power take-off on the energy absorption of a reactively controlled one degree of freedom wave energy converter," *Applied Ocean Research*, vol. 48, pp. 236–243, 2014.

[17] S. H. Salter, "Wave power," *Nature*, vol. 249, no. 5459, pp. 720–724, 1974.

[18] K. Budal and J. Falnes, "A resonant point absorber of ocean-wave power," *Nature*, vol. 256, no. 5517, pp. 478–479, 1975.

[19] G. Bacelli and R. G. Coe, "Comments on control of wave energy converters," *IEEE Transactions on Control Systems Technology*, vol. 29, no. 1, pp. 478–481, 2021.

[20] R. Raye, C. Nichols, A. Bharath, C. Candon, and E. Baca, "Data acquisition and control for marine energy devices: Cost considerations," National Renewable Energy Laboratory, Golden, CO, Tech. Rep. NREL/TP-5700-90817, 2024.

[21] T. R. Kuphaldt, *Lessons in Industrial Instrumentation*, version 2.33 ed. Open textbook, Creative Commons Attribution 4.0 license, ibiblio.org/kuphaldt/socratic/sinst, 2024.

[22] M. D. Earle, "Nondirectional and directional wave data analysis procedures," National Data Buoy Center, National Oceanic and Atmospheric Administration, Stennis Space Center, MS, NDBC Technical Document 03-01, 2003. [Online]. Available: https://www.ndbc.noaa.gov/wavemeas.pdf

[23] H. Nademi, B. J. Galindez, M. Ross, and M. Lopez, "Experimental validation of a modular all-electric power take-off topology for wave energy converter enabling marine renewable energy interconnection," *Journal of Marine Science and Engineering*, vol. 12, no. 8, p. 1323, 2024.

[24] M. Leijon, C. Boström, O. Danielsson, S. Gustafsson, K. Haikonen, O. Langhamer, E. Strömstedt, M. Stålberg, J. Sundberg, O. Svensson, S. Tyrberg, and R. Waters, "Wave energy from the North Sea: Experiences from the Lysekil research site," *Surveys in Geophysics*, vol. 29, no. 3, pp. 221–240, 2008.

[25] K. Stouffer, M. Pease, C. Tang, T. Zimmerman, V. Pillitteri, S. Lightman, A. Hahn, S. Saravia, A. Sherule, and M. Thompson, "Guide to operational technology (OT) security," National Institute of Standards and Technology, Gaithersburg, MD, Special Publication 800-82r3, 2023.

[26] T. Brekken, "Applied research and development to support open-water testing at PacWave, task 7: WEC system control for marine growth and electrical faults," Oregon State University, Corvallis, OR, Final Technical Report DOE-OSU-EE0009969-7, 2025.

5.10 Exercises

5.1 Concept check · 2 min

The chapter calls the force that captures the most energy from an irregular sea anticausal. What makes it so?

(a) The probe stands 30 m upstream, so its record reaches the controller late

(b) The drive's current loop lags the command, so the force must be asked for early

(c) The optimal velocity is the excitation through a filter whose response is even in time

(d) The end-stops bind only in waves that have not yet reached the buoy

5.2 Concept check · 1 min

In case 4 latching captures 1.236 kWh against the tuned damper's 0.747 kWh, although the brake holds the buoy still 43 % of the time. Why does it capture more?

(a) The meter credits the work the brake absorbs during each hold

(b) Holding the buoy stops it radiating for the rest of each wave period

(c) The brake raises the force rating of the generator while it holds

(d) Released at the right moment, the buoy moves while the wave force is with it

5.3 Concept check · 2 min

The energy the generator absorbs over a plan, $\sum_k f_k \Delta x_k$, is bilinear in force and motion, yet the MPC of Equation (5.13) is a convex quadratic program. Why?

(a) The model's energy balance turns it into terms with non-negative weights, because $b_1 a_1 > 0$

(b) The hard force bound $|f_k| \le F_{lim}$ removes the negative curvature of the bilinear term

(c) The slack price $\rho_2 = 10^{10}\,\mathrm{J/m^2}$ outweighs the bilinear term in the Hessian

(d) The 30 move blocks reduce the decision variables until no indefinite direction is left

5.4 Theory and calculation · 6 min

The buoy is a vertical cylinder of radius $a = 2.5\,\mathrm{m}$ and draft $d = 4\,\mathrm{m}$ in sea water of density $\rho = 1025\,\mathrm{kg/m^3}$, with $g = 9.81\,\mathrm{m/s^2}$. Its added mass at infinite frequency is the hemisphere's, $m_\infty = \rho \pi a^3/3$.

(a) Compute the displaced mass m, the hydrostatic stiffness k_h, the added mass m_∞ and the undamped natural period $T_n = 2\pi\sqrt{(m+m_\infty)/k_h}$. *Checkpoint:* 80.5 t, 197.4 kN/m, 16.8 t and 4.41 s.

(b) The dominant roots of the characteristic quartic of Section 5.4 are $-0.0612 \pm 1.4353i\,\mathrm{s^{-1}}$. Compute the damped period, the damping ratio and the ratio of one swing's amplitude to the one before. *Checkpoint:* 4.378 s, 0.043 and 0.76.

5.5 Theory and calculation · 8 min

Use the two-state radiation model of Equations (5.2) and (5.3) with $b_1 = 15\,908.67\,\mathrm{N/m}$, $a_1 = 1.408\,497\,\mathrm{s^{-1}}$ and $a_0 = 1.699\,333\,\mathrm{s^{-2}}$, and the masses of the previous exercise, at the wave period of 9 s.

(a) Compute the radiation damping $B(\omega)$, the added mass $a(\omega)$ and the reactance $X_i(\omega)$ of Equation (5.10). *Checkpoint:* 4.48 kN s/m, 24.7 t and −209.4 kN s/m.

(b) Compute the damping $|Z_i|$ that a damper alone should apply and the stiffness $K_{pto} = \omega X_i$ of the complex conjugate. *Checkpoint:* 209.4 kN s/m and −146.2 kN/m.

(c) In a regular 9 s wave, what fraction of the complex-conjugate power $|F|^2/(8B)$ does the best damper alone take? Use Equation (5.11). *Checkpoint:* 0.042.

5.6 Theory and calculation · 5 min

The MPC charges reactive power through the term $c\,(f-\hat{B}v)^2$ with $c = (1/\eta_{PTO}-1)/(4\hat{B})$, where v is the velocity over the step.

(a) Show that $(f-\hat{B}v)^2 + 4\hat{B}fv = (f+\hat{B}v)^2$, and conclude that $(f-\hat{B}v)^2/(4\hat{B}) \geq \max(-fv, 0)$ for any f, v and $\hat{B} > 0$. *Checkpoint:* The inequality holds with equality when $f = -\hat{B}v$.

(b) Take $\hat{B} = 215\,\mathrm{kN\,s/m}$ and $\eta_{PTO} = 0.8$. For $f = -100\,\mathrm{kN}$ and $v = 0.5\,\mathrm{m/s}$, compare the MPC's charge $(1/\eta_{PTO}-1)(f-\hat{B}v)^2/(4\hat{B})$ with the meter's extra charge $(1/\eta_{PTO}-1)\max(-fv, 0)$. Repeat for $f = 100\,\mathrm{kN}$ at the same velocity. *Checkpoint:* 12.52 kW against 12.50 kW, and 0.016 kW against zero.

5.7 App challenge · 8 min

Load scenario 2, Passive damping: tuned to the sea. The damper is set to 40 kN s/m in a 1.5 m, 9 s sea. Use the default seed, run at 10× (30 s of wall time) to the pause at 300 s.

(a) Run as shipped. Read the Captured energy tile (energy and capture width ratio), the Peak PTO force tile and the stroke used on the End-stop contacts tile. *Checkpoint:* 0.47 kWh, 13 %, 44 kN and 1.31 m.

(b) Press Reset, press Tune to the sea and run again. Read the PTO damping it set and the same tiles. *Checkpoint:* 215 kN s/m, 0.77 kWh, 21 %, 123 kN and 0.79 m.

(c) Exercise 5.5 gives $|Z_i| = 209.4\,\mathrm{kN\,s/m}$ at 9 s. Read the note the helper writes and explain why it set 215 kN s/m. Then explain why the damper that takes more resists harder and lets the buoy move less. *Checkpoint:* The note reads $\hat{T}_p$ 9.1 s and $|Z_i(\hat{\omega}_p)| = 213\,\mathrm{kN\,s/m}$, rounded to the dial's 5 kN s/m.

5.8 App challenge · 9 min

Use the default seed, the speed 10×, and runs of 300 s to the pause. Read the Captured energy tile after each run.

(a) Load scenario 5, The anticausal optimum: a perfect forecast against none. Run it as shipped, with the Forecast horizon at 0 s. Set the Forecast horizon to 4.0 s, press Reset and run again. Also read the Peak PTO force and Reactive energy tiles of the second run. *Checkpoint:* 0.86 kWh, then 2.71 kWh at 294 kN with 0.51 kWh pushed back.

(b) Load scenario 6, The real forecast: energy against horizon. Run it as shipped, with the real forecast at 4.0 s. Set the Forecast horizon to 1.0 s, press Reset and run again. *Checkpoint:* 2.52 kWh, then 1.82 kWh.

(c) Compute the ratio of the perfect forecast's energy at 4 s to none, the share of the perfect forecast's energy that the real forecast keeps at 4 s, and explain why the real forecast loses more at long leads than at short ones. *Checkpoint:* 3.1 and 93 %, within one in the last digit.

5.9 App challenge · 8 min

Load the challenge, *Challenge · twenty minutes through three seas*. It uses one recorded sea at seed 3. Set the speed to 30× (40 s of wall time per run) and run each policy to the end at 1200 s. Read the Captured energy, End-stop contacts and Challenge target tiles.

(a) Run the shipped damper of 170 kN s/m. *Checkpoint:* 8.91 kWh, 23 contacts, not met.

(b) Set the Strategy to Predictive (MPC), keep the Real (AR) forecast at 4.0 s, set the Survival threshold to 3.3 m, press Reset and run. Also read the Reactive energy tile. *Checkpoint:* 10.89 kWh, no contact, met, with 1.19 kWh pushed back.

(c) Lower the Survival threshold to 3.0 m, press Reset and run again. Explain the result, and say what the 18.585 kWh that the MPC captures without survival, with two contacts, tells an engineer. *Checkpoint:* 8.02 kWh, no contact, not met.

5.10 Application area · 3 min

Reactive control in case 3 captures 1.330 kWh at a peak force of 215 kN, and the tuned damper 0.767 kWh at 123 kN. The reactive run pushes 0.088 kWh back into the sea.

(a) A linear generator is sized, and largely priced, by the largest force it must make. Compute the energy captured per kilonewton of peak force for each controller. *Checkpoint:* 6.24 Wh per kilonewton for the damper and 6.19 Wh for reactive control.

(b) The meter credits absorbed power in full and charges reactive power at $1/\eta_{PTO}$ with $\eta_{PTO} = 0.8$. How much did the reactive run absorb in all, before the charge? *Checkpoint:* 1.440 kWh.

5.11 Application area · 4 min

The chapter's hydrodynamics are teaching values. A matched-eigenfunction solution of the same cylinder gives an added mass at infinite frequency of 30.4 t against 16.8 t and a natural period of 4.67 s against 4.38 s.

(a) The latching rule of Section 5.5 sets $T_L = (\hat{T}_{m01} - T_n)/2$ with $\hat{T}_{m01} = 0.8348\,\hat{T}_p$ and $T_n = 4.41$ s. For a peak period of 10 s, compute the hold with the app's T_n and with the cylinder's 4.67 s. *Checkpoint:* 1.97 s and 1.84 s.

(b) In which direction would the complex-conjugate stiffness K_{pto} at 9 s move on the real cylinder, and why does the chapter say that its ranking of the controllers still holds? *Checkpoint:* Toward zero, a smaller negative spring.

5.12 Review the agent · 5 min

An AI assistant is asked how to set the damper of scenario 2 and replies as follows. "At a period of 9 s the radiation resistance of this buoy is $B(\omega) = 4.5\,\mathrm{kN\,s/m}$. By the maximum power transfer theorem the load must match the source resistance, so set the PTO damping to 5 kN s/m, the nearest dial value. This is the textbook optimum for a point absorber, and it will capture far more than the 215 kN s/m that Tune to the sea sets." Find the flaw and say how you would check it.